Cell Stem Cell, Volume *20*

Supplemental Information

Two-Way Conversion between Lipogenic and Myogenic Fibroblastic Phenotypes Marks the Progression and Resolution of Lung Fibrosis

Elie El Agha, Alena Moiseenko, Vahid Kheirollahi, Stijn De Langhe, Slaven Crnkovic, Grazyna Kwapiszewska, Djuro Kosanovic, Felix Schwind, Ralph T. Schermuly, Ingrid Henneke, BreAnne MacKenzie, Jennifer Quantius, Susanne Herold, Aglaia Ntokou, Katrin Ahlbrecht, Rory E. Morty, Andreas Günther, Werner Seeger, and Saverio Bellusci

SUPPLEMENTAL FIGURES & TEXT

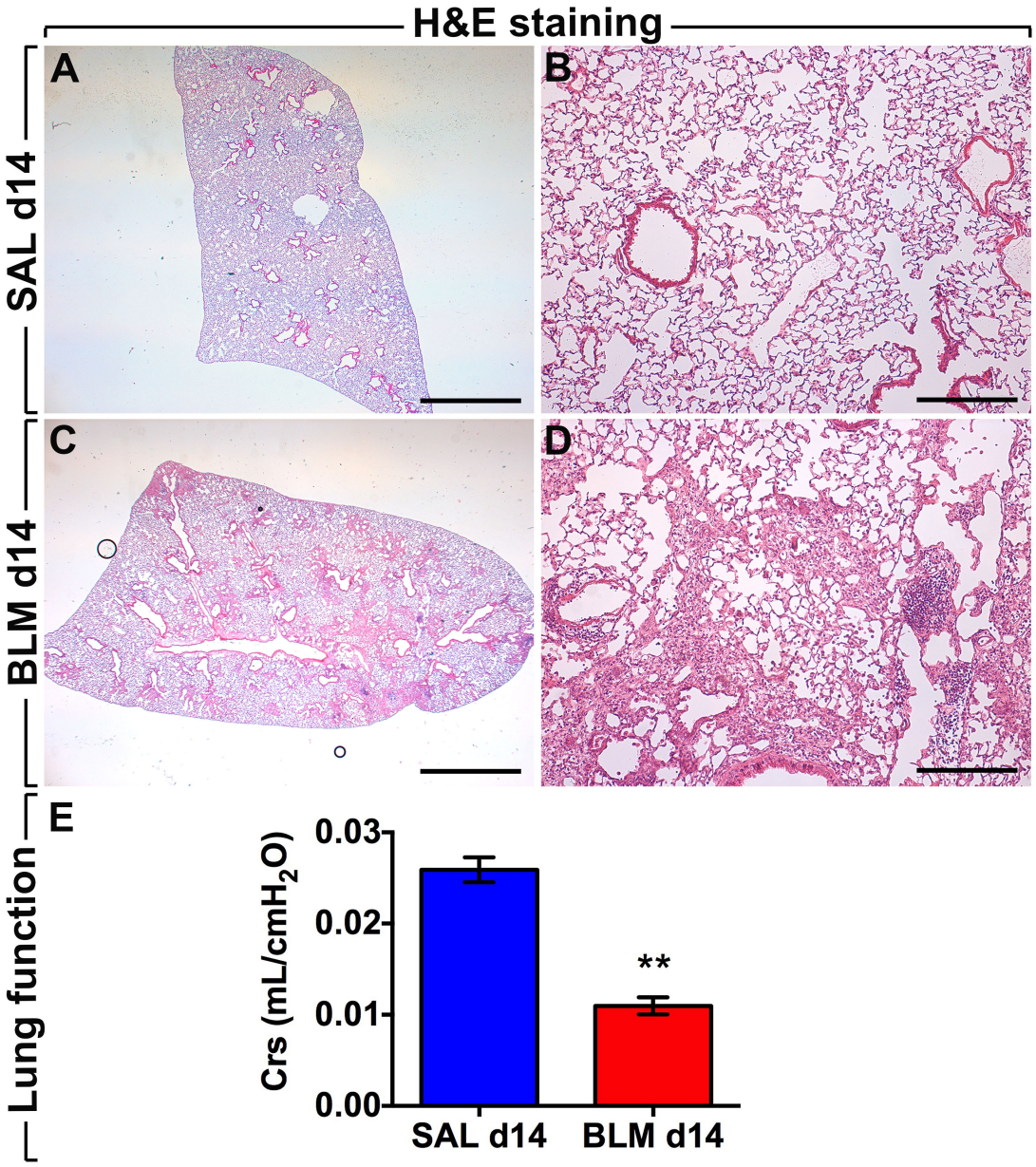

Supplemental Figure S1, related to Figure 1, Validation of bleomycin-induced lung fibrosis in *Acta2-Cre-ERT2; tdTomato*^{flox} mice at 14 d.p.i. **(A)** H&E stain of a saline-treated lung at 14 d.p.i. A higher magnification is shown in **(B). (C)** H&E stain of a bleomycin-treated lung at 14 d.p.i. A higher magnification is shown in **(D). (E)** Lung function measurement showing decreased compliance in bleomycin-treated lungs compared to controls. Scale bars: (A,C) 2 mm, (B,D) 200 μm. SAL d14 *n*=4, BLM d14 *n*=7, 'n' represents biological replicates. ** *P*<0.01.

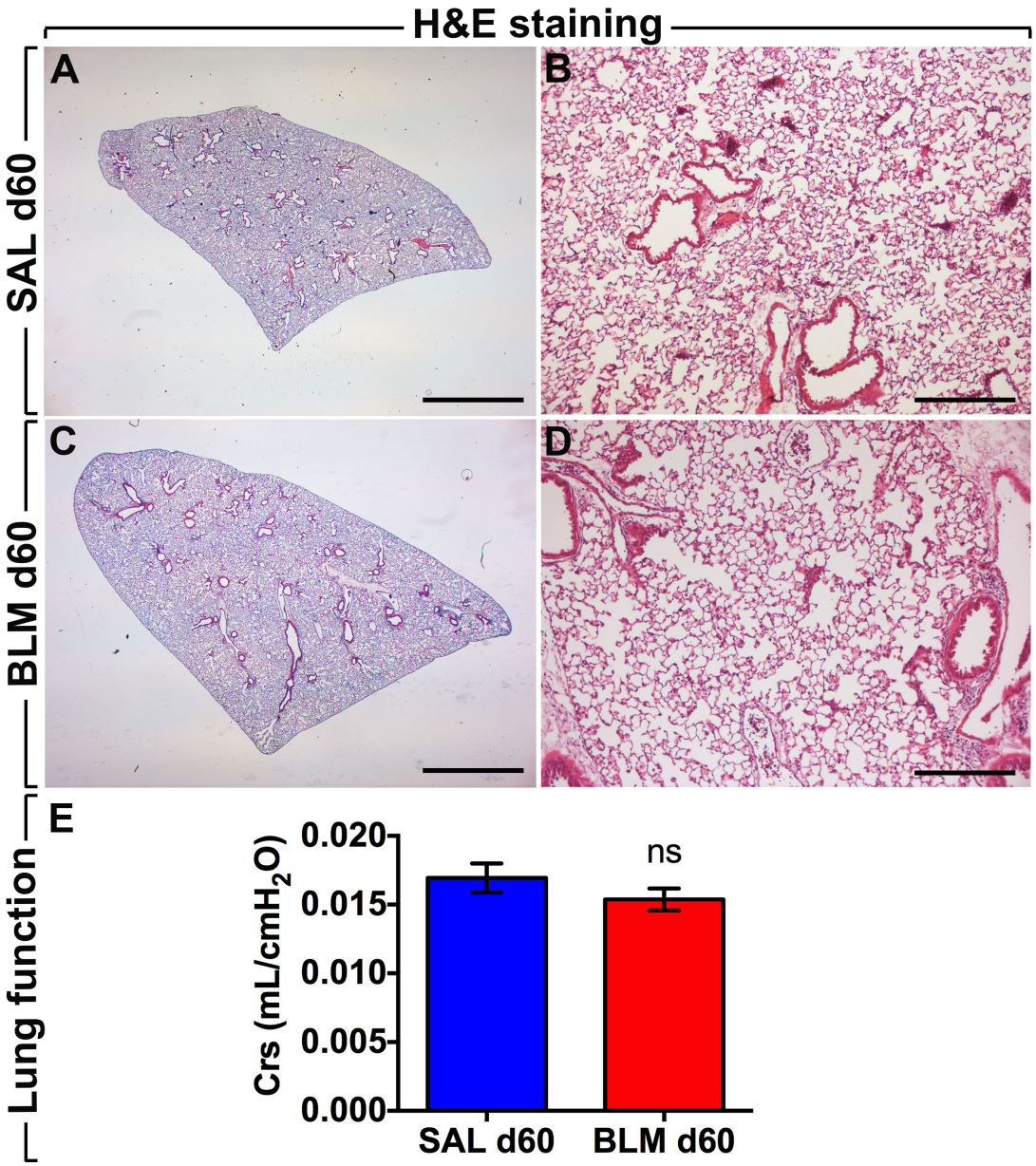

Supplemental Figure S2, related to Figures 2 and 3, Validation of fibrosis resolution in *Acta2-Cre-ERT2; tdTomato*^{flox} mice at 60 d.p.i. (A) H&E stain of a saline-treated lung at 60 d.p.i. A higher magnification is shown in **(B). (C)** H&E stain of a bleomycin-treated lung at 60 d.p.i. A higher magnification is shown in **(D). (E)** Lung function measurement showing no difference in compliance in bleomycin-treated lungs compared to controls. Scale bars: (A,C) 2 mm, (B,D) 200 μm. *n*=3 per group, 'n' represents biological replicates.

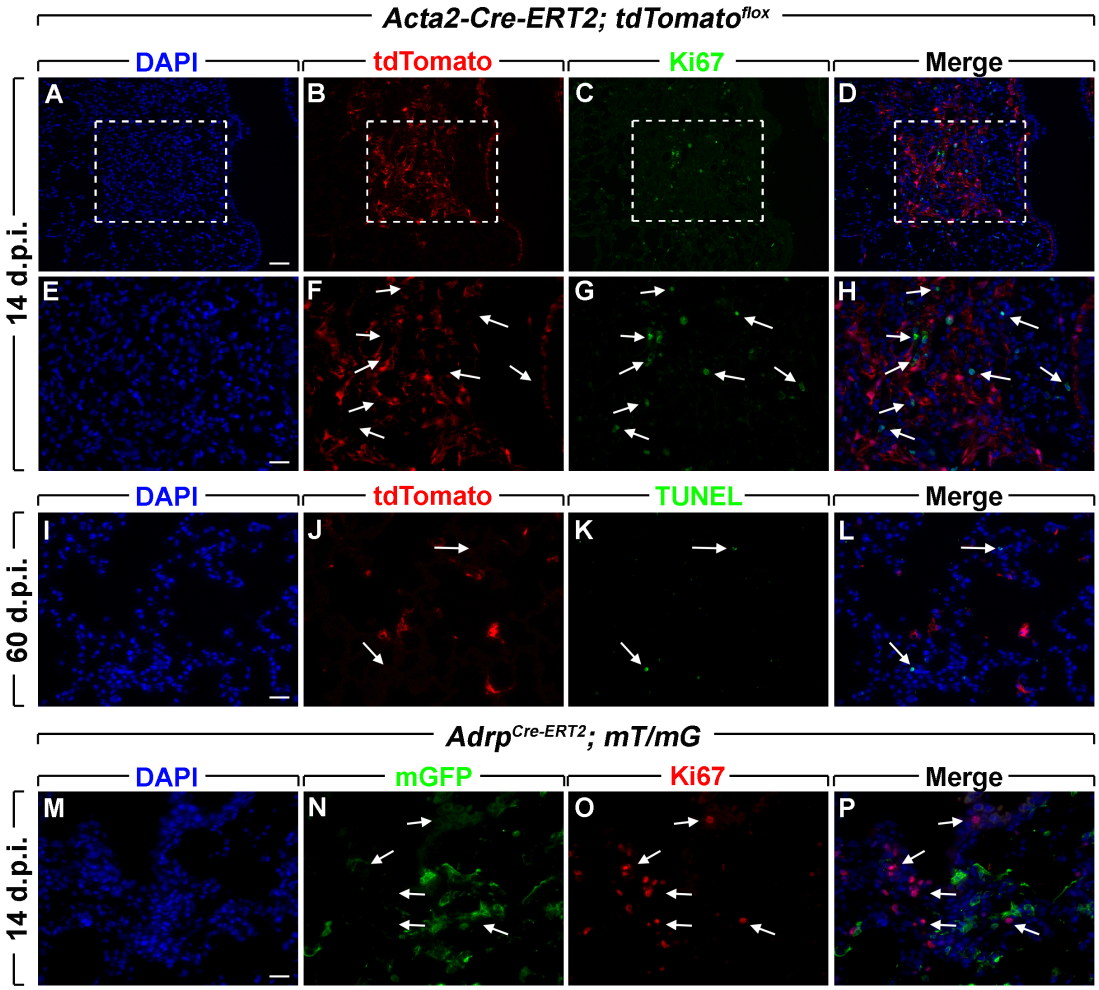

Supplemental Figure S3, related to Figures 2, 3 and 4, Analysis of proliferation and apoptosis in lineage-labeled cells at the peak of fibrosis and during the resolution phase. (A-D) Immunofluorescent staining of bleomycin-treated *Acta2-Cre-ERT2; tdTomato*^{flox} lungs at 14 d.p.i. showing DAPI, tdTomato and Ki67 single channels in addition to a merged image. High magnification images of the regions marked by the boxes are shown in **(E-H).** White arrows mark proliferating cells. Note the absence of co-localization between the lineage label and Ki67 stain. **(I-L)** TUNEL staining of *Acta2-Cre-ERT2; tdTomato*^{flox} lungs at 60 d.p.i. showing the absence of apoptosis in lineage-labeled cells. White arrows mark apoptotic cells. **(M-P)** Immunofluorescent staining of bleomycin-treated *Adrp*$^{Cre-ERT2}$*; mT/mG* lungs at 14 d.p.i. showing DAPI, mGFP and Ki67 single channels in addition to a merged image. White arrows mark proliferating cells. Note the absence of co-localization between the lineage label and Ki67 stain. Scale bars: (A-D) 50 μm, (E-P) 25 μm. (A-H) *n*=3, (I-L) *n*=2, (M-P) *n*=3, 'n' represents biological replicates.

A **TGFβ pathway analysis for *Adrp$^{Cre\text{-}ERT2}$; mT/mG* (BLM d14 vs. SAL d14)**

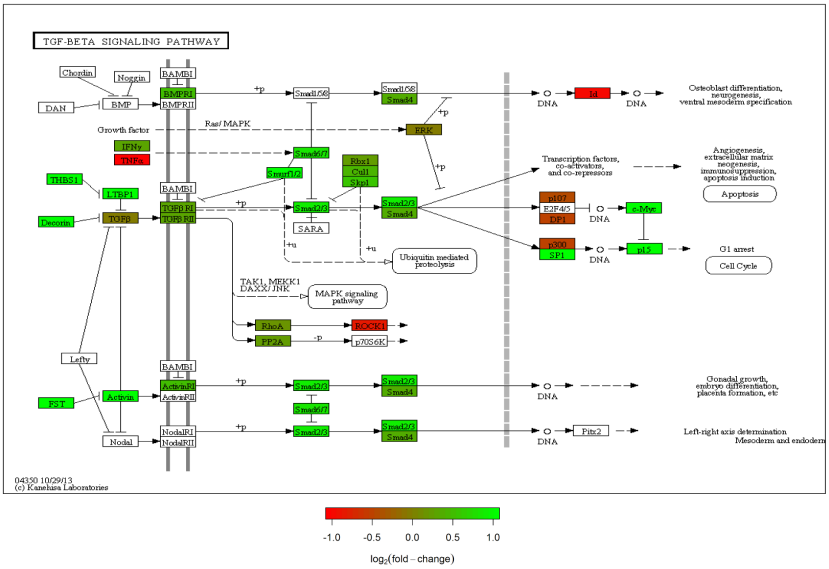

B **PPARγ pathway analysis for *Acta2-Cre-ERT2; tdTomato^{flox}* (BLM d60 vs. BLM d14)**

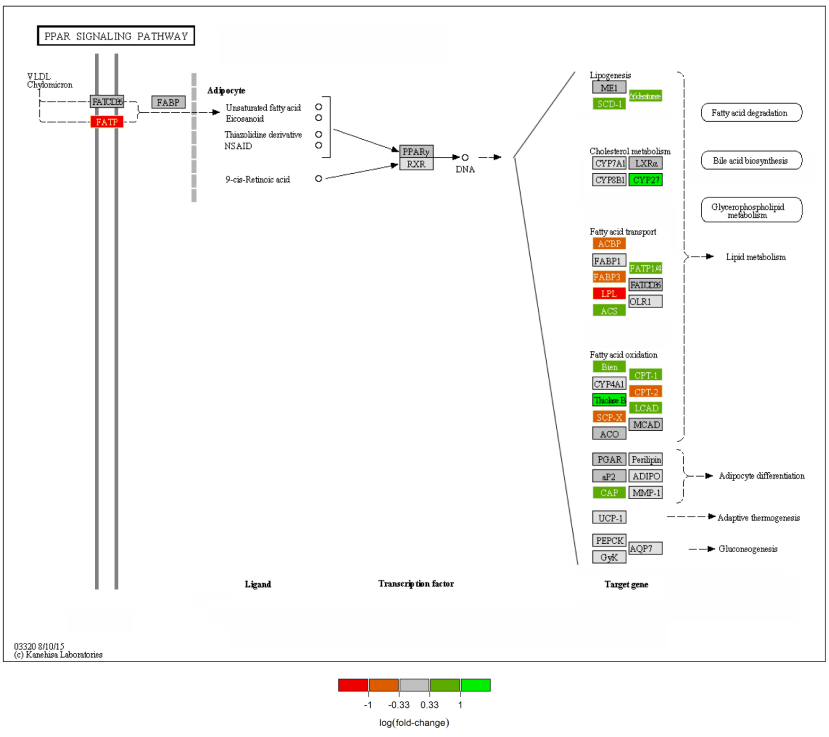

Supplemental Figure S4, related to Figures 2, 3 and 4, Signaling pathway analysis on lineage-labeled cells isolated from *Adrp$^{Cre\text{-}ERT2}$; mT/mG* and *Acta2-Cre-ERT2; tdTomato^{flox}* mice during fibrosis formation and resolution. (A) Analysis of gene arrays performed on sorted mGFP^{+} cells showing activation of the TGFβ signaling pathway in lipofibroblast-derived cells during fibrosis formation. **(B)** Analysis of gene arrays performed on sorted tdTomato^{+} cells showing activation of the PPARγ signaling pathway in activated myofibroblast descendants following fibrosis resolution. (A) *n*=3 per group, (B) BLM d14 *n*=3, BLM d60 *n*=2, 'n' represents biological replicates.

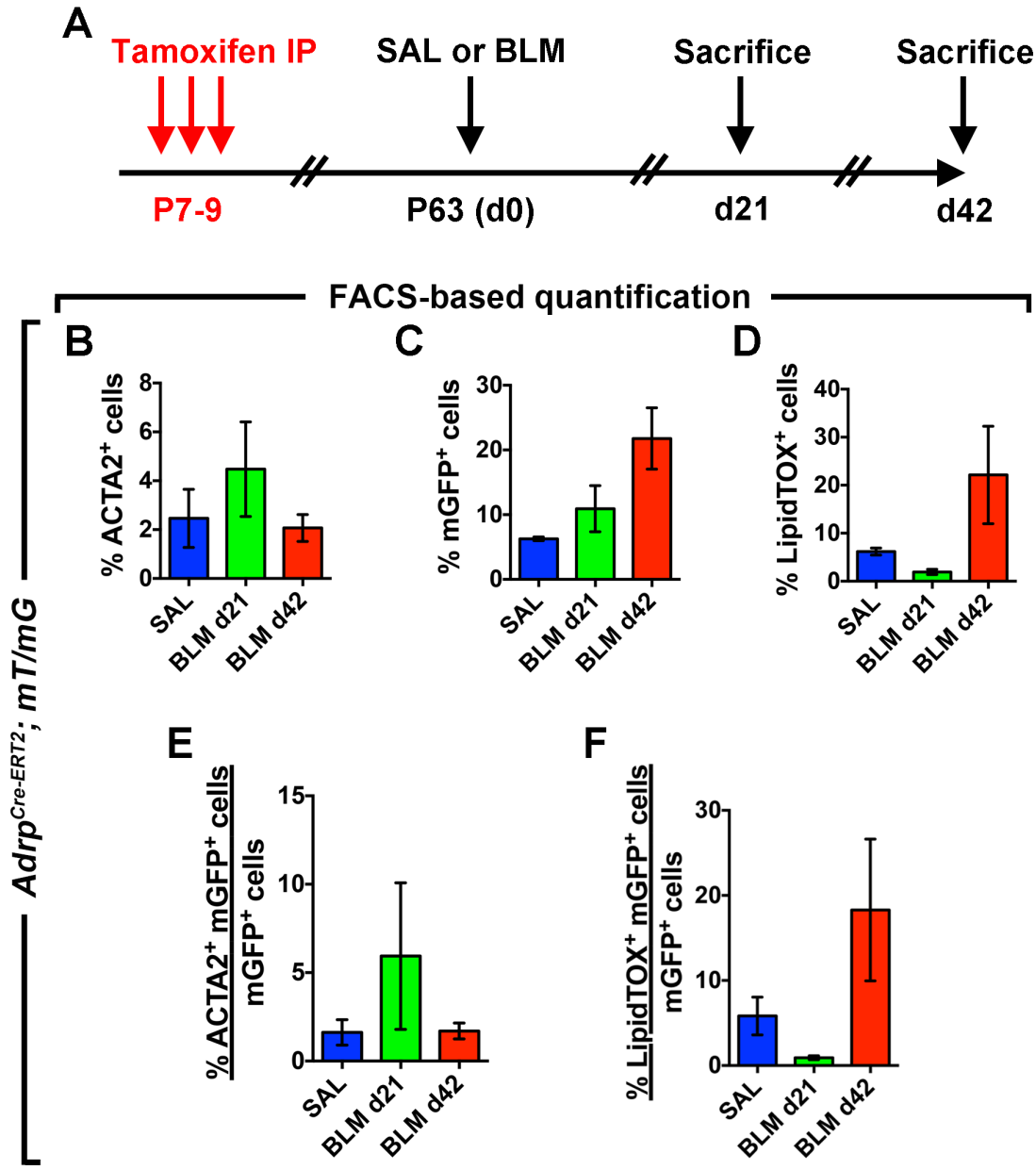

Supplemental Figure S5, related to Figure 4, Lipofibroblasts are maintained, regain their lipid content and lose ACTA2 expression during the resolution phase of lung fibrosis. (A) Pre-existing lipofibroblasts were labeled by three intraperitoneal injections of tamoxifen at P7, 8 and 9, before animals were challenged with saline or bleomycin at P63. **(B-F)** FACS-based quantification shows a transient increase in the number of ACTA2$^+$ cells (B) and a transient loss of LipidTOX$^+$ cells at 21 d.p.i. (D). mGFP$^+$ cells are maintained at 21 d.p.i., and tend to be more abundant at 42 d.p.i. (C). (E,F) Lipofibroblast-derived cells acquire ACTA2 expression and lose their lipid content at 21 d.p.i. and then lose ACTA2 expression and reacquire lipid content at 42 d.p.i. IP: Intraperitoneal injection. SAL d14 *n*=3, BLM d21 *n*=3, BLM d42 *n*=4, 'n' represents biological replicates.

Supplemental Table S1, related to STAR Methods, Primers used in this study.

Mouse primers	
Acta2 Fwd	5'-ACTCTCTTCCAGCCATCTTTCA-3'
Acta2 Rev	5'-ATAGGTGGTTTCGTGGATGC-3'
Adrp Fwd	5'-CTCCACTCCACTGTCCACCT-3'
Adrp Rev	5'-GCTTATCCTGAGCACCCTGA-3'
Col1a1 Fwd	5'-CCAAGAAGACATCCCTGAAGTCA-3'
Col1a1 Rev	5'-TGCACGTCATCGCACACA-3'
Fgf10 Fwd	5'-ATGACTGTTGACATCAGACTCCTT-3'
Fgf10 Rev	5'-CACTGTTCAGCCTTTTGAGGA-3'
Pparg Fwd	5'-GAAAGACAACGGACAAATCACC-3'
Pparg Rev	5'-GGGGGTGATATGTTTGAACTTG-3'
Human primers	
ACTA2 Fwd	5'-CTGTTCCAGCCATCCTTCAT-3'
ACTA2 Rev	5'-TCATGATGCTGTTGTAGGTGGT-3'
ADRP Fwd	5'-TCAGCTCCATTCTACTGTTCACC-3'
ADRP Rev	5'-CCTGAATTTTCTGATTGGCAC-3'
C/EBPa Fwd	5'-GACATCAGCGCCTACATCG-3'
C/EBPa Rev	5'-GGCTGTGCTGGAACAGGT-3'
COL1A1 Fwd	5'-ATGTTCAGCTTTGTGGACCTC-3'
COL1A1 Rev	5'-CTGTACGCAGGTGATTGGTG-3'
FGF10 Fwd	5'-GAAGGAGAACTGCCCGTACA-3'
FGF10 Rev	5'-GGCAACAACTCCGATTTCTACT-3'
PPARg Fwd	5'-TCTGCAAACATATCACAAGAAATGAC-3'
PPARg Rev	5'-ATATCAAAGGAGTGGGAGTGG-3'